JOURNAL OF BIOMOLECULAR STRUCTURE AND DYNAMICS
https://doi.org/10.1080/07391102.2020.1804458

Structural insight to hydroxychloroquine-3C-like proteinase complexation from SARS-CoV-2: inhibitor modelling study through molecular docking and MD-simulation study

Soumita Mukherjee[a], Subrata Dasgupta[a], Tapasendra Adhikary[b], Utpal Adhikari[a] and Sujit Sankar Panja[a]

[a]Department of Chemistry, National Institute of Technology-Durgapur, Durgapur, West Bengal, India; [b]Department of Metallurgical & Materials Engineering, Indian Institute of Technology, Kharagpur, West Bengal, India

Communicated by Ramaswamy H. Sarma

ABSTRACT

The spread of novel coronavirus strain, Severe Acute Respiratory Syndrome 2 (SARS-CoV-2) causes Coronavirus disease (COVID-19) has now spread worldwide and effecting the entire human race. The viral genetic material is transcripted and replicated by 3 C-like protease, as a result, it is an important drug target for COVID-19. Hydroxychloroquine (HCQ) report promising results against this drug target so, we perform molecular docking followed by MD-simulation studies of HCQ and modelled some ligand (Mod-I and Mod-II) molecules with SARS-CoV-2-main protease which reveals the structural organization of the active site residues and presence of a conserve water-mediated catalytic triad that helps in the recognition of Mod-I/II ligand molecules. The study may be helpful to gain a detailed structural insight on the presence of water-mediated catalytic triad which could be useful for inhibitor modelling.

ABBREVIATIONS: COVID-19: Coronavirus Disease-2019; HCQ: Hydroxychloroquine; Mpro: Main protease; MD: Molecular Dynamics; MM-PBSA: Molecular Mechanics Poisson-Boltzmann Surface Area; ns: nanosecond; ps: picosecond; K: kelvin; SARS-CoV-2: Severe Acute Respiratory Syndrome 2

ARTICLE HISTORY
Received 29 May 2020
Accepted 28 July 2020

KEYWORDS
COVID-19; SARS-CoV-2; Hydroxychloroquine; catalytic triad; conserved water molecule

Introduction

The novel coronavirus outbreak was first reported in Wuhan city of China on December 2019 which causes the Coronavirus disease 2019 (COVID-19) (Sohrabi et al., 2020) is now spread worldwide and effecting the entire human race. The virus strain responsible for this ongoing pandemic is called Severe Acute Respiratory Syndrome 2 (SARS-CoV-2) which is the successor to SARS-CoV-1 and also related to Middle East coronavirus (MERS-CoV) (Petrosillo et al., 2020) having the highest mortality rate among all human coronaviruses (Elfiky & Azzam, 2020). All three viruses have a common host and have originated from bats (Hemida & Ba Abduallah, 2020; Hu et al., 2015). The spread of SARS-CoV-1 (in the year 2002) and MERS-CoV (in the year 2012) to humans is believed to be through civet cats (Wang & Eaton, 2007) and camels (Azhar et al., 2014) unfortunately the mediator for SARS-CoV-2 is still unknown but researchers suspect that ant-eating pangolins may be responsible for this spread as Pangolin-CoV is 91.02% identical to SARS-CoV-2 (T. Zhang et al., 2020).

During this pandemic several drug targets have been identified which includes RNA-dependent RNA polymerase (Anwar et al., 2020; Arya & Dwivedi, 2020; Babadaei, Hasan, Vahdani, et al., 2020; Elfiky, 2020b), Spike glycoprotein (Adeoye et al., 2020; Basit et al., 2020; de Oliveira et al., 2020; Elfiky, 2020a; Sinha et al., 2020; Wahedi et al., 2020), Angiotensin-converting enzyme 2 (ACE2) (Abdelli et al., 2020; Ahmad et al., 2020; Babadaei, Hasan, Bloukh, et al., 2020; Hasan et al., 2020; V. Kumar, Dhanjal, Bhargava, et al., 2020; Veeramachaneni et al., 2020; Wahedi et al., 2020), Nucleocapsid protein (Sarma et al., 2020), Papain-like proteinase (Quimque et al., 2020), 3 C-like proteinase (Das et al., 2020; Enmozhi et al., 2020; Islam et al., 2020; Umesh et al., 2020) and they may be useful for drug development. However, design and search of multi-epitope vaccine candidate molecules have also been initiated in different laboratories (Abraham Peele et al., 2020; Enayatkhani et al., 2020).

The SARS-CoV-2 is a positive-sense single-stranded RNA virus (Hendaus, 2020; Lu et al., 2020) which utilizes non-structural protein (nsp) complexes for the process of transcription and replication in human cells. The replicase polyprotein is processed by viral protease known as Papain like protease (PLP) and 3 C-like protease (3CL protease) or also known as the main protease which is attractive drug targets for the present pandemic COVID-19 (Al-Khafaji et al., 2020; Bhardwaj et al., 2020; Gupta et al., 2020; Gyebi et al., 2020; A. Kumar, Choudhir, Shukla, et al., 2020; D. Kumar, Kumari, Jayaraj, et al., 2020; Mittal et al., 2020; Sk et al., 2020) and is most widely studied target for COVID-19 which also

CONTACT Sujit Sankar Panja sujit.panja@gmail.com Department of Chemistry, National Institute of Technology-Durgapur, M.G. Avenue, Durgapur, West Bengal 713209, India.

Supplemental data for this article can be accessed online at https://doi.org/10.1080/07391102.2020.1804458.

remains conserved among several coronaviruses (CoV), so we select it for our study. The X-ray crystal structures of SARS-CoV-2 3CL-protease were surveyed from RCSB Protein Data Bank (Berman et al., 2000; Burley et al., 2019) which showed the protein consists of three domains. The Domains I (consisting of 1–99 amino acids), Domain II (consisting of 100–183 amino acids), and Domain III (consisting of 200–306 amino acids) in which domain I contributed His41 and domain II contributed Cys145 together forming a catalytic dyad found in entire CoV superfamily. However, the third catalytic residue is missing and the position seems to be occupied by an invariant water molecule (L. Zhang, Lin et al., 2020). The Domain I is connected to Domain III through a connecting loop consisting of 184–199 amino acid residues (Figure 1(a)). The ligand-binding site is comprised of Thr26, His41, Phe140, Asn142, Gly143, Cys145, His163, His164, Met165, Glu166, Gln189 and Thr190 residues as can be seen in 6lu7 crystal structure(Jin et al., 2020) (Figure 1(b)).

The Hydroxychloroquine is an FDA approved drug that has been used to treat malaria(Al-Bari, 2015; Tanenbaum & Tuffanelli, 1980) rheumatoid arthritis(Rynes, 1988), chronic discoid lupus erythematosus(Wahie & Meggitt, 2013), and systemic lupus erythematosus(Chew et al., 2020). During this pandemic emergency, HCQ has been showing promising effect in the treatment of COVID-19 (Boopathi et al., 2020; Hendaus & Jomha, 2020) so, several theoretical and experimental studies are conducted to understand the inhibiting mechanism of this malarial drug to SARS-CoV-2 (Amin & Abbas, 2020; Beura & Chetti, 2020; Beura & Prabhakar, 2020; Devaux et al., 2020; Gautret et al., 2020).

The X-ray crystallographic studies have indicated the inhibitor/drug binding site on 3CL-protease which helps in identification for new potential inhibitor molecules, consequently a large number of theoretical studies are conducted that attempts identification of repurposing drugs for COVID-19 (Aanouz et al., 2020; Choudhury, 2020; Elmezayen, Al-Obaidi, Şahin, & Yelekçi, 2020; Joshi et al., 2020; M. T. Khan et al., 2020; R. J. Khan et al., 2020; S. A. Khan, Zia, Ashraf, Uddin, & Ul-Haq, 2020; V. Kumar, Dhanjal, Kaul, Wadhwa, & Sundar, 2020; Lobo-Galo, Terrazas-López, Martínez-Martínez, & Díaz-Sánchez, 2020; Mahanta et al., 2020; Muralidharan, Sakthivel, Velmurugan, & Gromiha, 2020; Pant, Singh, Ravichandiran, Murty, & Srivastava, 2020). In our study we carefully investigated the catalytic and inhibitor binding site of 3CL-protease in the crystal and MD-simulated structures. We also report the binding mechanism and stabilization of Hydroxychloroquine with SARS-CoV-2 main protease through non-covalent interactions as well as attempt has been made to model some new structural analogs (Mod I and I′, Mod II and II′) and their recognition dynamics to conserved water-mediated catalytic triad.

Material and methods

The X-ray structures of some 3CL-protease from SARS-CoV-2 have been surveyed which were selected from RCSB Protein Data Bank (Supplementry material Table S1). The position and hydrogen bonding interaction of catalytic residues were examined using the UCSF Chimera program(Pettersen et al., 2004).

Ligand preparation

The ligand (HCQ, Mod I, Mod I′, Mod II, Mod II′) structures (Figure 2) were built by using the Gaussview program(Dennington et al., 2009). The structures were then subjected to geometry optimization with B3LYP/6-31G level of theory, solvation energies were added using the conductor-like Polarizable Continuum Models (CPCM). The partial atomic charges of the atoms were retained during classical MD-simulation. All the QM calculations were performed by using the Gaussian 09 package(Frisch et al. (2009) Gaussian 09 A.02).

Protein–ligand docking

The 3CL-protease has one ligand binding site which has been indicated in the X-ray crystallographic studies. Ligand–receptor docking was performed using Autodock Vina v.1.1.1 (Trott & Olson, 2009). The 6LU7 X-ray structure (excluding water and ligand molecules) was considered as a receptor. Two PDBQT files were generated for the receptor protein, one for rigid portion and another for flexible (His41 and Cys145) side chains using AutoDock Tools v.1.5.4 (Morris et al., 2009) by assigning Kollman united atom charges (Weiner et al., 1984). The QM optimized structures of ligand molecules (HCQ and Mod-I, I′, II, II′) were converted into PDBQT files after including their partial atomic charges using the Gasteiger method (Gasteiger & Marsili, 1980). Grid point spacing was set at 1 Å and 20 grid points were taken in each direction. As the location of the ligand binding site was already known (PDB id: 6LU7), so grid box was centered at that site. Vina automatically calculated the grid map for searching. All other docking parameters were assigned to their default values. The docked structures were visually inspected and selected for further work. The ligand–receptor docking was also validated with DockThor (A receptor-ligand docking program) server (De Magalhães et al., 2014; Santos et al., 2020).

Molecular dynamics (MD) simulation

Molecular dynamics simulation was performed using NAMD v.2.12 (Kalé et al., 1999; Phillips et al., 2005) with the CHARMM36 force field(Brooks et al., 1983; Huang & MacKerell, 2013; MacKerell et al., 1998) . Then each structure was converted to Protein Structure File (PSF) by Automatic PSF Generation Plug-in within VMD program v. 1.9.2 (Humphrey et al., 1996). Subsequent energy minimization was performed by the conjugate gradient method. The process was conducted in two successive stages; initial energy minimization was performed for 2000 steps by fixing the backbone atoms, followed by a final minimization for 5000 steps that were carried out for all atoms of the system to ensure the removal of any residual steric clashes. Then the energy minimized structures were simulated at constant temperature (310 K) and

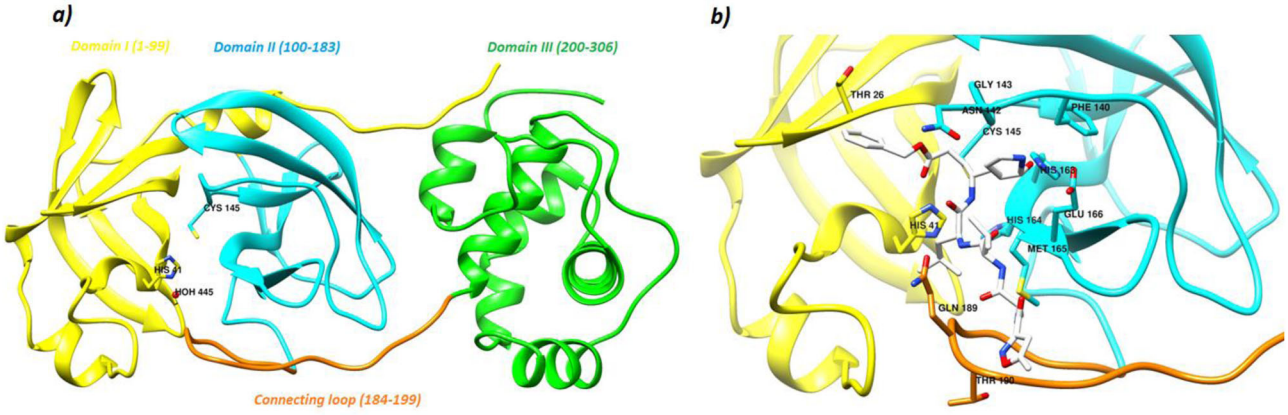

Figure 1. The structural representation of SARS-CoV-2 Mpro (PDB Id:6LU7). a) Domain I, II III, and the connecting loop are shown by yellow, cyan, green and orange colours respectively. This colouring scheme for the protein has been maintained in the entire manuscript. The catalytic dyad (His41 and Cys145) and the invariant water molecule (HOH445) are shown here. b) The active site residues with the N3-inhibitor molecule (carbon atom is shown with white). The carbon atoms of amino acids are shown with their representative domain colour.

pressure (1 atm) by Langevin dynamics (Gullingsrud et al., 2001) using periodic boundary condition. The Particle Mesh Ewald method was applied for full-electrostatics and the Nose–Hoover Langevin piston method was used to control the pressure and dynamical properties of the barostat(Feller et al., 1995). All-atom molecular dynamics simulation for 100 ns was carried out for HCQ, Mod I, and Mod II docked 3CL-protease structure. The atomic coordinates of simulated structures were recorded at every 2 ps for further analysis.

MM-PBSA calculation

The ligand-receptor binding energies were calculated by Molecular Mechanics-Poisson Boltzmann Surface Area (MM-PBSA) method using Calculation of Free Energy (CaFE) program(Liu & Hou, 2016). It is capable of handling the simulation trajectories generated by various force field and is powered by VMD and NAMD. Three different energy terms are calculated by the MM-PBSA method which includes energy difference between the complex and separate receptor and ligand molecule in the gas phase from NAMD. Then, the polar solvation free energy was calculated using the APBS program(Baker et al., 2001) and finally, the difference of solvent-accessible surface area (SASA) is measured and the nonpolar solvation free energy was estimated. The binding energies are calculated by using the following equation:

$$\Delta G_{bind} = G_{complex} - (G_{receptor} + G_{ligand})$$

The binding energies of the ligand-receptor complexes were calculated at 20 ns interval over the simulation trajectories.

Results and discussion

The analysis of 3CL-protease crystal structures from SARS-CoV-2 showed that the His 41 of Domain I lies close to Cys145 of Domain II which together form the catalytic dyad. An invariant water molecule, HOH445 (W1) is positioned within hydrogen bond distance to $His41_{ND1}$, $Arg40_{NB}$, $His164_{ND1}$, and $Asp187_{OD2}$ atoms (Figure 3).

The Root Mean Square Deviation (RMSD) of the protein backbone (Cα) atoms (Figure 4) show that the Mod I/Mod II complexed M^{Pro} structures are more stable than the HCQ complexed structure whereas, the Root Mean Square Fluctuation (RMSF) curve shows the active site residues in all the three complexes are stable with small fluctuations at N and C-terminal region of the protein. All the ligand-protein complexes show similar deviation and fluctuation validating the consistency of the simulation trajectories.

Molecular docking and simulation studies of hydroxychloroquine (HCQ) with 3CLpro

The optimized structure of HCQ was docked in 6lu7 crystal structure, the ligand molecule binds to a groove on the surface of the protein with binding energy ∼-5.4 kcal/mol. The catalytic dyad (His41 and Cys145) interacts with the si-face (under the aromatic ring) of the ligand molecule through non-covalent interaction. The His41 endowed parallel displaced π···π interaction with aromatic ring 1 of HCQ and the Cys145 shown S-H···π interaction with aromatic ring 2 of HCQ. The $Thr24_{OG1}$ located at the entrance of the inhibitor binding site is stabilized by the O21 hydroxyl group of HCQ through hydrogen bond interaction (Supplementry material Figure S1).

During simulation, the hydrogen bond interaction between $Cys145_{SG}$ and $His41_{NE2}$ is ranging from 3.1 to 3.3 Å and the average H-bond interaction of W1 water center to $His41_{ND1}$, $Arg40_{NB}$, $His164_{ND1}$, and $Asp187_{OD2}$ atoms are observed to be ∼ 3.0–3.3, 3.1–3.4, 2.8–3.4, 2.7–3.2 Å respectively (Figure 5).

A distorted trigonal pyramidal geometry has been observed around the W1 water center where $Arg40_{NB}$ and His164 at the apex position and His41, His164, and Asp187 are present at the three corners of the plane (Figure 6) with ∼100% residential frequency. In this HCQ complex structure, the $Cys145_{SG}$ atom is observed to lie near C8 and C9 carbon centers with ∼3.88 and 3.72 Å distance respectively suggesting these two centers may be important for inhibitor

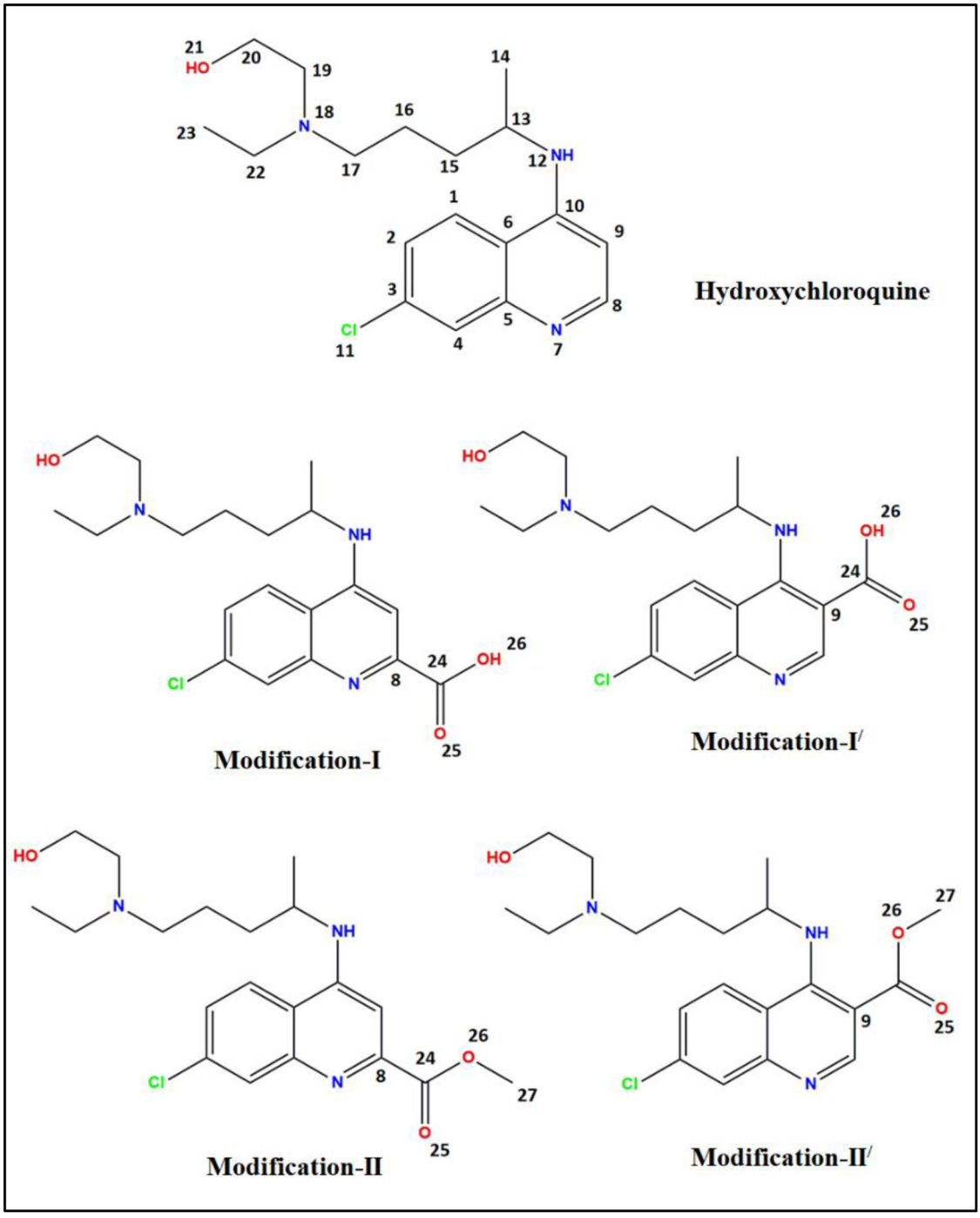

Figure 2. Chemical structures of HCQ and modified ligand molecules included in this study.

modeling so, these carbon centers were modified by substituting with different functional groups for easy nucleophilic attack by Cys145 catalytic residue.

Molecular docking and simulation studies of modified inhibitor molecules with 3CL-protease

Observing the structural arrangement and interaction of His41 and Cys145 with HCQ, some ligand molecules were modelled (Figure 2) and docked into the inhibitor binding cavity of the 6lu7 crystal structure. The docked structures of modified ligand molecules (Mod I, I/, II, and II/) win the 6lu7 crystal structure are shown in Supplementry material Figure S2.

The binding energies (B.E.) for Mod I and Mod II are observed to be −6.1 and −5.5 kcal/mol whereas that of Mod I/and Mod II/are −5.4 and −5.3 kcal/mol respectively. The results indicate that the modification of HCQ at the C8 position is energetically favourable compared to the C9-position. Moreover, we may say the formation of carbocation at C8-position of Modified ligand molecules would be more stable than at C9-position due to –I effect of N7-atom in the aromatic ring of the ligand molecule so, Mod I and Mod II structures were selected for further MD-simulation studies.

The molecular dynamics simulation of Mod I and Mod II complexed 6lu7 structure shows that the $Cys145_{SG}$ lies in close proximity to O25 atom of the ligand with average distance ranging from 3.2 to 3.7 Å for Mod I and 3.5 to 4.0 Å for Mod II complexed structure (Figure 7 and 8). The hydrogen bond interaction between the catalytic dyad $Cys145_{SG}\cdots His41_{NE2}$ varies from 3.2 to 3.5 Å. The W1 water molecule forms strong hydrogen bond interaction with $His41_{ND1}$ and $Asp187_{OD2}$ thus bridging the gap between these two residues. The $His41_{ND1}\cdots W1$ distance ranges from ~3.1 to 3.4 Å and 3.0 to 3.3 Å whereas that of $W1\cdots Asp187_{OD2}$ ranges from 2.7 to 2.9 and 2.7 to 3.0 Å for the respective Mod I and Mod II complex structures (Figure 7 and 8).

In classical proteases (like chymotrypsin, trypsin or elastase), the catalytic triad is made up of an acid, base and a nucleophile but in coronavirus main proteases (SARS-CoV-2 Mpro (PDB Id 6lu7), SARS-CoV Mpro (PDB Id 2zu5) and MERS-CoV Mpro (PDB Id 5wkk)) presence of water-mediated Aspartic acid residue along with base (His) and nucleophile (Cys) seem to be unique and reflecting the formation of water-mediated catalytic triad so, the occupation of W1 water center adjacent to the base (His41) and its recognition to Asp187 through $Asp187_{OD2}\cdots W1\cdots His41_{NE2}$ interaction could be an evolutionary change in the catalytic site of CoV-Mpro for unknown reasons.

During simulation, the recognition of Asp187 to Mod I/II is observed to made through $Asp187_{OD2}\cdots W1\cdots His41_{ND1/NE2}\cdots Cys145_{SG}\cdots$ Mod I/II (O25) path. The carbonyl oxygen (O25) is stabilized by amide backbone atoms of Cys145, Ser144, and Gly143 residues (Figure 9).

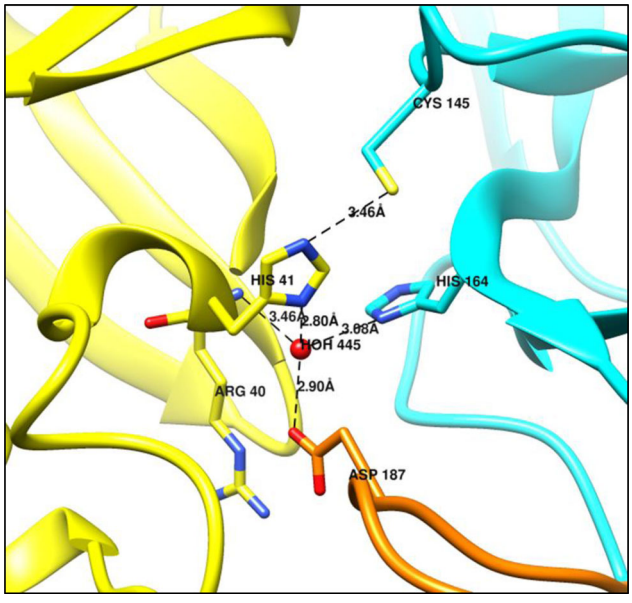

Figure 3. The interaction of $His41_{ND1}$, $Arg40_{NB}$, $His164_{ND1}$, and $Asp187_{OD2}$ residues with an invariant water molecule through hydrogen bond interaction. The hydrogen bonds are shown by dotted lines.

MM-PBSA binding free energy

The binding free energies of the ligand-receptor complexes by the MM-PBSA method (Table 1) are calculated. The final binding energy is the cumulative sum of Electrostatic, Van der Waal, Polar solvation, and SASA energies which show that the Mod II structure has better binding energies when compared to Mod I and HCQ molecules. The Mod I structure shows low binding and electrostatic energies compared to the HCQ complex structure. The Mod II complexed structure shows high binding energy of ~−213.09 kcal/mol at 80–100ns time interval.

So, analyses of crystal and ligand-bound simulated structures from SARS-CoV-2 Mpro a mechanism has been proposed which may shed some light on the mechanistic role of the above residues in ligand complexed Mpro structures (Figure 10).

In SARS-CoV-2 Mpro the catalytic triad is made up of Cys145, His41, and Asp187 residues, a catalytic water (HOH445) which is associated with His41 and Asp187 through hydrogen bond interaction. Initially, His41 abstracts a proton from Cys145 making it a better nucleophile (cysteine thiyl radical, $CysS^{-}$) for attack on the carbonyl carbon (C24) of the ligand molecule. The Asp187 and HOH445 anchor the His41 molecule to its correct conformation during the formation of transition state complexes. The reaction is

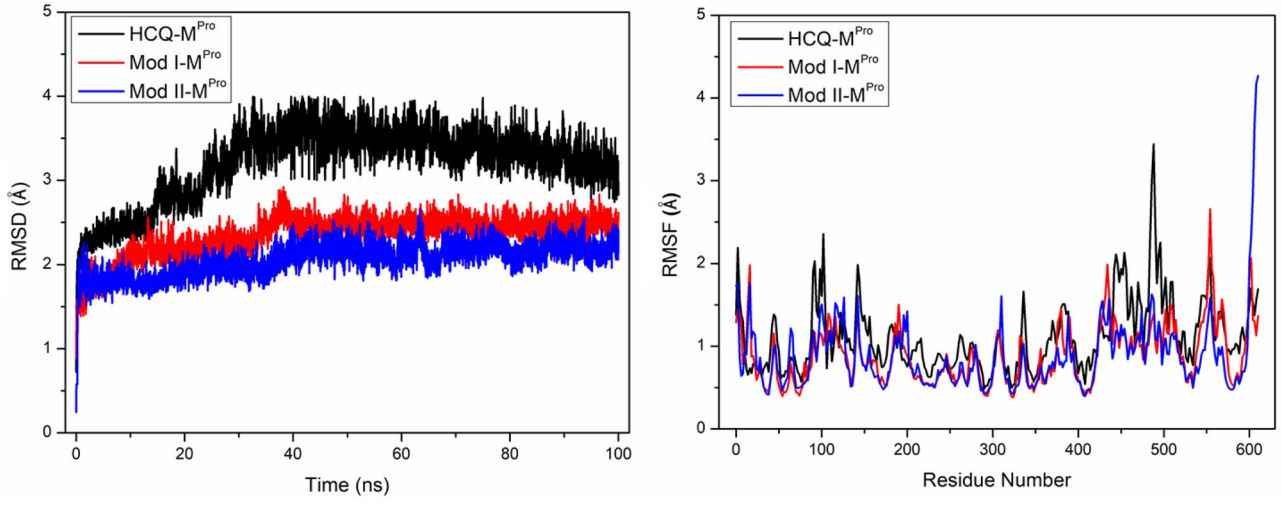

Figure 4. The Root Mean Square Deviation (RMSD) and Root Mean Square Fluctuation (RMSF) curves of the protein backbone (C_α) atoms during MD-simulation.

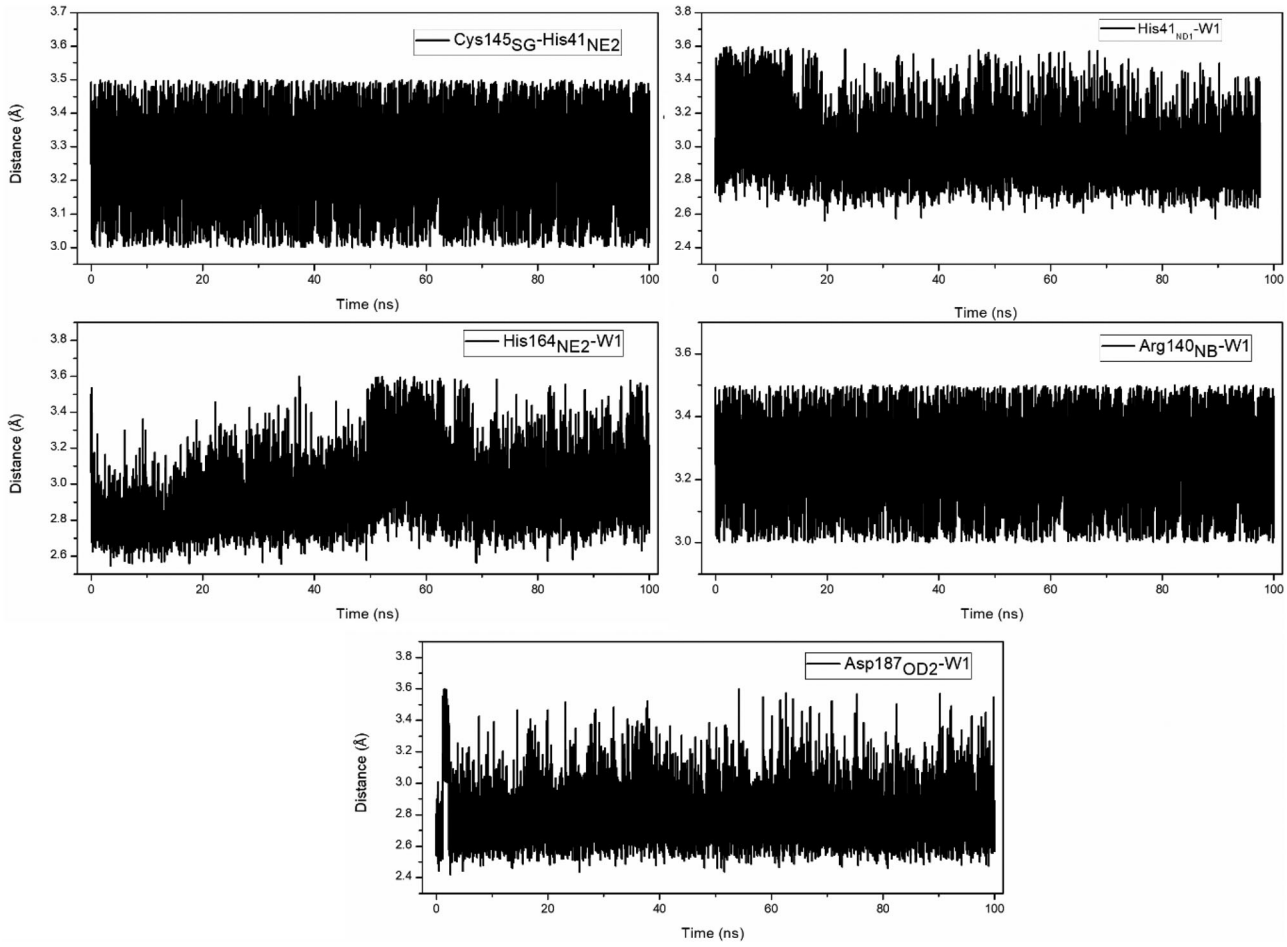

Figure 5. Hydrogen bond interaction between different residues in HCQ-SARS-CoV-2 Mpro during MD-simulation.

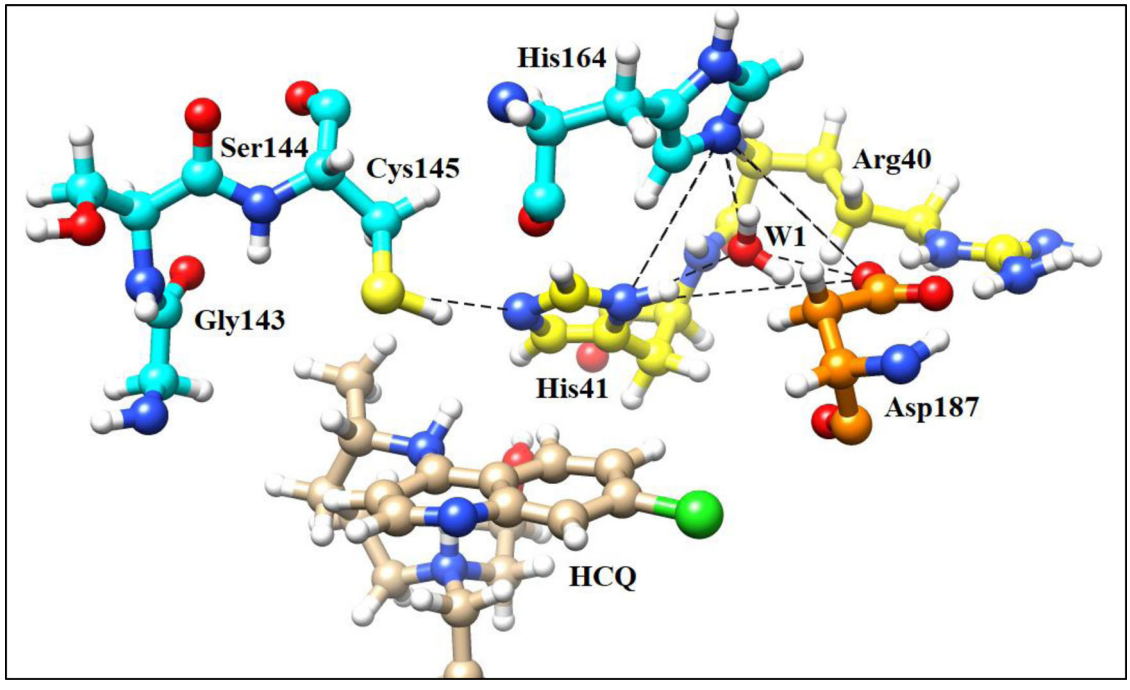

Figure 6. The hydrogen bonding geometry around W1 water center involving His41, Arg40, His164, and Asp187 residues during MD-simulation.

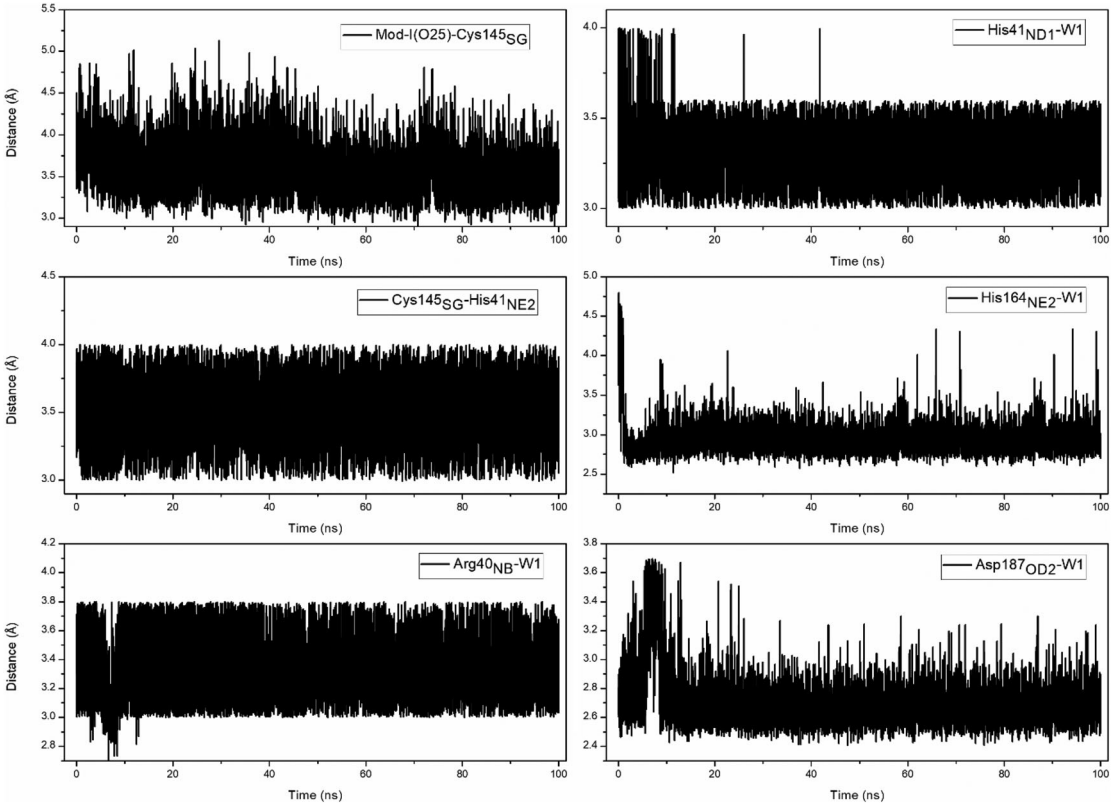

Figure 7. Hydrogen bonding interaction between the different residues in Mod-I-SARS-CoV-2 Mpro during MD-simulation.

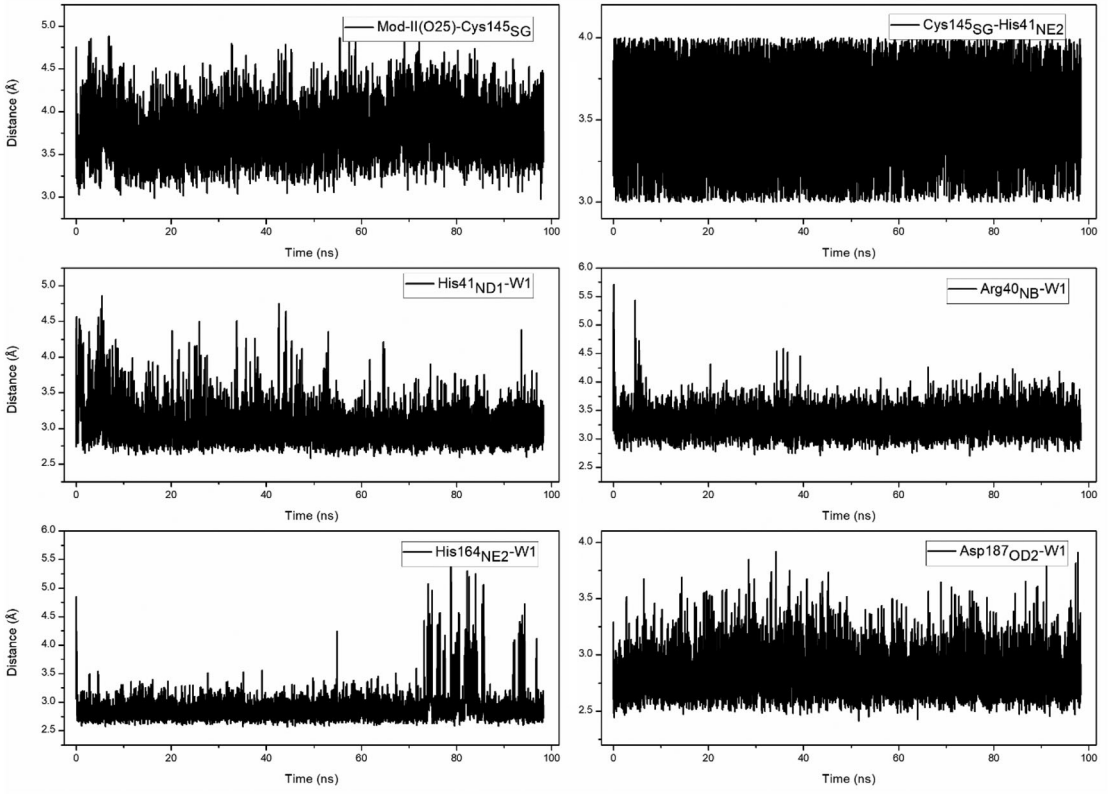

Figure 8. Hydrogen bond interaction between different residues in Mod-II-SARS-CoV-2 Mpro during MD-simulation.

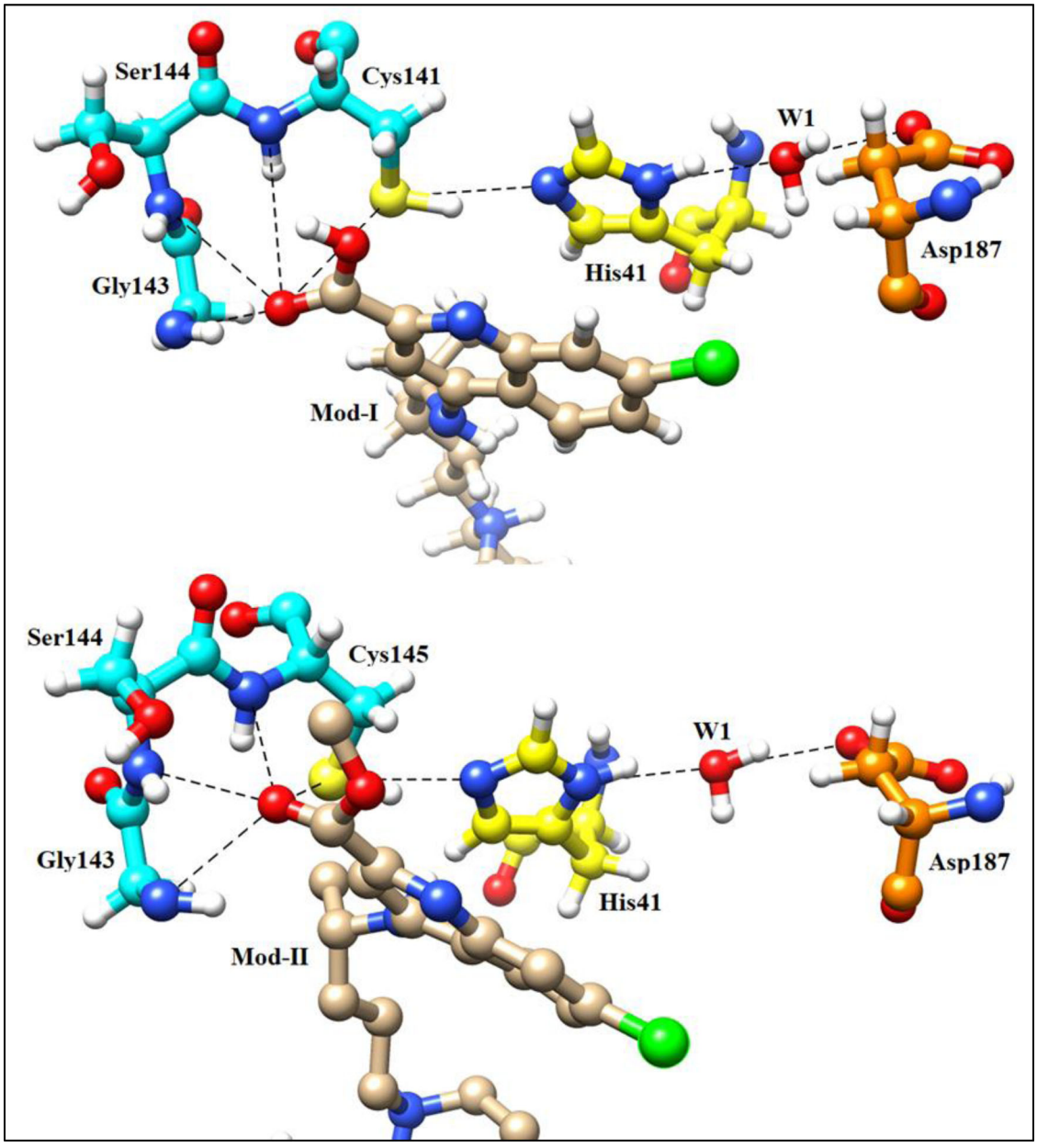

Figure 9. Recognition of Mod-I/II to Cys145, His41, Asp187 residues and W1(HOH445) water center.

Table 1. The MM-PBSA binding free energy calculation for HCQ, Mod I, and Mod II-M^{Pro} complex structures during MD-simulation. All the given energies are in kcal/mol.

Complex	Time (ns)	$\Delta E_{Electrostatic}$	$\Delta E_{Van\ der\ Waal}$	ΔE_{polar}	SASA	$\Delta E_{binding}$
HCQ-M^{Pro}	20	−130.55 +/- 3.47	−35.81 +/- 3.74	36.24 +/- 2.95	−40.70 +/- 3.65	−170.82 +/- 3.45
	40	−137.29 +/- 1.38	−34.66 +/- 1.33	33.57 +/- 1.16	−39.44 +/- 1.30	−177.82 +/- 1.29
	60	−151.44 +/- 3.22	−32.61 +/- 3.12	29.57 +/- 2.83	−37.27 +/- 3.10	−191.75 +/- 3.06
	80	−150.93 +/- 2.72	−33.08 +/- 2.87	31.86 +/- 1.89	−37.74 +/- 2.84	−189.89 +/- 2.58
	100	−153.59 +/- 4.95	−32.72 +/- 2.59	30.96 +/- 1.65	−37.34 +/- 2.57	−192.69 +/- 2.94
Mod I-M^{Pro}	20	−115.93 +/- 3.93	−36.14 +/- 3.98	39.10 +/- 0.30	−40.84 +/- 4.06	−153.81 +/- 3.06
	40	−124.83 +/- 2.16	−39.37 +/- 1.99	42.01 +/- 1.54	−44.48 +/- 1.96	−166.67 +/- 1.91
	60	−125.62 +/- 2.54	−39.60 +/- 4.23	46.33 +/- 2.55	−44.70 +/- 4.21	−163.59 +/- 3.38
	80	−125.24 +/- 4.47	−39.10 +/- 2.34	45.54 +/- 3.30	−44.22 +/- 2.34	−163.02 +/- 3.11
	100	−135.22 +/-2.66	−35.09 +/- 2.09	39.68 +/- 2.44	−40.04 +/-2.06	−170.67 +/- 2.31
Mod II-M^{Pro}	20	−148.43 +/- 6.29	−48.22 +/- 3.38	51.47 +/- 4.73	−54.02 +/- 3.42	−199.2 +/- 4.45
	40	−157.48 +/- 2.42	−45.61 +/- 1.89	43.25 +/- 0.98	−51.15 +/- 1.89	−210.99 +/- 1.79
	60	−157.20 +/- 1.06	−45.32 +/- 2.80	43.34 +/- 0.91	−50.92 +/- 2.76	−210.1 +/- 1.88
	80	−155.53 +/- 4.03	−46.20 +/- 2.80	42.28 +/- 0.85	−51.86 +/- 2.79	−211.31 +/- 2.61
	100	−157.45 +/- 1.00	−45.88 +/- 3.41	41.87 +/- 2.64	−51.63 +/- 3.38	−213.09 +/- 2.60

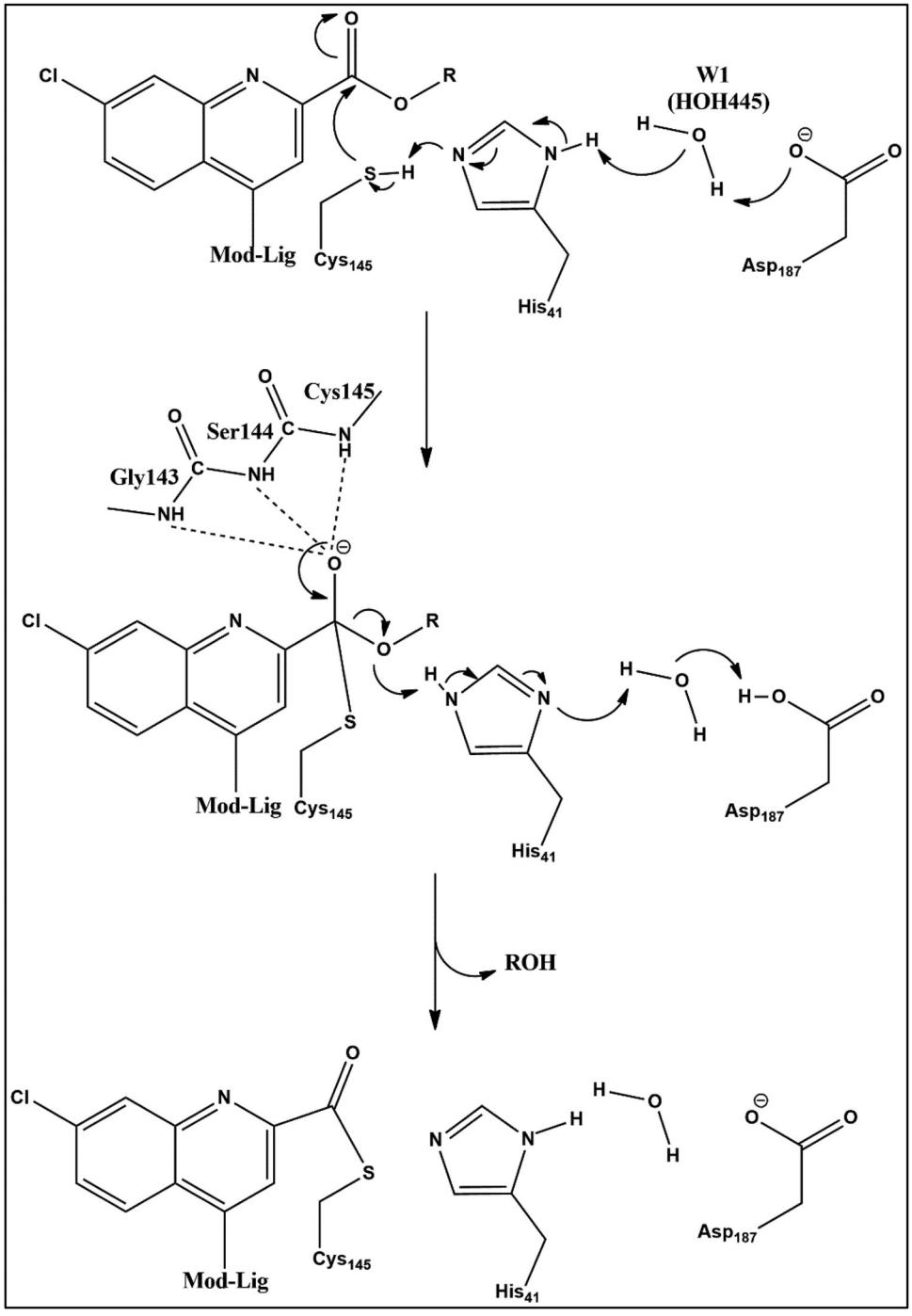

Figure 10. Proposed mechanism of action in SARS-CoV-2 Mpro.

followed by the formation of a tetrahedral intermediate where the oxyanion group of the intermediate is stabilized by amide backbone atoms of Gly143, Cys145, and Ser144 residues. Finally, the ROH product molecule is released from the reaction medium by the formation of a stable Mod-lig-Cys145 adduct.

Conclusion

The Molecular docking followed by MD-simulation of the HCQ complexed structure of SARS-CoV-2 Mpro reveals the binding of this ligand molecule on the surface of the protein structure near to the catalytic dyad (His41 and Cys145). The Cys145 is observed to lie near the C8 and C9 centers of the ligand molecule which encouraged us to modify these centers by addition of –COOH and –$COOCH_3$ functional groups. The modified ligand molecules (Mod I and Mod II) are found to have higher binding energy towards the inhibitor binding domain compared to their counter partners (Mod I′and Mod II′). During the simulation of Modified ligand molecules with SARS-CoV-2 Mpro, the Cys145 is observed to be perfectly positioned near the C24 atom of ligand molecules thus suggesting the possibility of a nucleophilic attack to this site

during catalysis. The W1 water center hydrogen-bonded to $His41_{ND1}$ seems to be crucial for the recognition of ligand molecules to catalytic dyad and Asp187 (located on the connecting loop between Domain I and Domain III) through Mod-I/II(O25)···Cys145···$His41_{NE2/ND1}$···W1···$Asp187_{OD2}$ interaction. So, from the results, it may be presumed that the Asp187 may function as the third catalytic residue where W1 water center maintains the structural recognition of this catalytic triad.

Acknowledgements

SM, SD, UA, and SSP acknowledge the National Institute of Technology (Government of India)–Durgapur for providing research facilities at the Department of Chemistry, NIT Durgapur. All the authors acknowledge Mr. Swarnendu Gupta for computational assistance.

Disclosure statement

No potential conflict of interest was reported by the authors.

References

Aanouz, I., Belhassan, A., El-Khatabi, K., Lakhlifi, T., El-Ldrissi, M., & Bouachrine, M. (2020). Moroccan medicinal plants as inhibitors against SARS-CoV-2 main protease: Computational investigations. *Journal of Biomolecular Structure and Dynamics*. 1-9. https://doi.org/10.1080/07391102.2020.1758790

Abdelli, I., Hassani, F., Bekkel Brikci, S., & Ghalem, S. (2020). In silico study the inhibition of angiotensin converting enzyme 2 receptor of COVID-19 by Ammoides verticillata components harvested from Western Algeria. *Journal of Biomolecular Structure and Dynamics*. 1-14. https://doi.org/10.1080/07391102.2020.1763199

Abraham Peele, K., Srihansa, T., Krupanidhi, S., Vijaya Sai, A., & Venkateswarulu, T. C. (2020). Design of multi-epitope vaccine candidate against SARS-CoV-2: A in-silico study. *Journal of Biomolecular Structure and Dynamics*. 1-9. https://doi.org/10.1080/07391102.2020.1770127

Adeoye, A. O., Oso, B. J., Olaoye, I. F., Tijjani, H., & Adebayo, A. I. (2020). Repurposing of chloroquine and some clinically approved antiviral drugs as effective therapeutics to prevent cellular entry and replication of coronavirus. *Journal of Biomolecular Structure and Dynamics*, 1–11. https://doi.org/10.1080/07391102.2020.1765876

Ahmad, S., Abbasi, H. W., Shahid, S., Gul, S., & Abbasi, S. W. (2020). Molecular docking, simulation and MM-PBSA studies of nigella sativa compounds: A computational quest to identify potential natural antiviral for COVID-19 treatment. *Journal of Biomolecular Structure and Dynamics*. 1-9. https://doi.org/10.1080/07391102.2020.1775129

Al-Bari, A. A. (2015). Chloroquine analogues in drug discovery: New directions of uses, mechanisms of actions and toxic manifestations from malaria to multifarious diseases. *The Journal of Antimicrobial Chemotherapy*, *70*(6), 1608–1621. https://doi.org/10.1093/jac/dkv018

Al-Khafaji, K., Al-Duhaidahawi, D., & Taskin Tok, T. (2020). Using integrated computational approaches to identify safe and rapid treatment for SARS-CoV-2. *Journal of Biomolecular Structure and Dynamics*, 1–9. https://doi.org/10.1080/07391102.2020.1764392

Amin, M., & Abbas, G. (2020). Docking study of Chloroquine and Hydroxychloroquine interaction with SARS-CoV-2 spike glycoprotein-An in silico insight into the comparative efficacy of repurposing antiviral drugs. *Journal of Biomolecular Structure and Dynamics*. 1-13. https://doi.org/10.1080/07391102.2020.1775703

Anwar, F., Altayb, H. N., Al-Abbasi, F. A., Al-Malki, A. L., Kamal, M. A., & Kumar, V. (2020). Antiviral effects of probiotic metabolites on COVID-19. *Journal of Biomolecular Structure and Dynamics*. 1-10. https://doi.org/10.1080/07391102.2020.1775123

Arya, A., & Dwivedi, V. D. (2020). Synergistic effect of vitamin D and remdesivir can fight COVID-19. *Journal of Biomolecular Structure and Dynamics*, 1–2. https://doi.org/10.1080/07391102.2020.1773929

Azhar, E. I., El-Kafrawy, S. A., Farraj, S. A., Hassan, A. M., Al-Saeed, M. S., Hashem, A. M., & Madani, T. A. (2014). Evidence for camel-to-human transmission of MERS coronavirus. *The New England Journal of Medicine*, *370*(26), 2499–2505. https://doi.org/10.1056/NEJMoa1401505

Babadaei, M. M. N., Hasan, A., Bloukh, S. H., Edis, Z., Sharifi, M., Kachooei, E., & Falahati, M. (2020). The expression level of angiotensin-converting enzyme 2 determines the severity of COVID-19: Lung and heart tissue as targets. *Journal of Biomolecular Structure and Dynamics*, 1–7. https://doi.org/10.1080/07391102.2020.1767211

Babadaei, M. M. N., Hasan, A., Vahdani, Y., Bloukh, S. H., Sharifi, M., Kachooei, E., Haghighat, S., & Falahati, M. (2020). Development of remdesivir repositioning as a nucleotide analog against COVID-19 RNA dependent RNA polymerase. *Journal of Biomolecular Structure and Dynamics*, 1–9. https://doi.org/10.1080/07391102.2020.1767210

Baker, N. A., Sept, D., Joseph, S., Holst, M. J., & McCammon, J. A. (2001). Electrostatics of nanosystems: Application to microtubules and the ribosome. *Proceedings of the National Academy of Sciences of the United States of America*, *98*(18), 10037–10041. https://doi.org/10.1073/pnas.181342398

Basit, A., Ali, T., & Rehman, S. U. (2020). Truncated human angiotensin converting enzyme 2; a potential inhibitor of SARS-CoV-2 spike glycoprotein and potent COVID-19 therapeutic agent. *Journal of Biomolecular Structure and Dynamics*, 1–10. https://doi.org/10.1080/07391102.2020.1768150

Berman, H. M., Westbrook, J., Feng, Z., Gilliland, G., Bhat, T. N., Weissig, H., Shindyalov, I. N., & Bourne, P. E. (2000). The Protein Data Bank. *Nucleic Acids Research*, *28*(1), 235–242. https://doi.org/10.1093/nar/28.1.235

Beura, S., & Chetti, P. (2020). In-silico strategies for probing chloroquine based inhibitors against SARS-CoV-2. *Journal of Biomolecular Structure and Dynamics*, 1–13. https://doi.org/10.1080/07391102.2020.1772111

Beura, S., & Prabhakar, C. (2020). In-silico strategies for probing chloroquine based inhibitors against SARS-CoV-2. *Journal of Biomolecular Structure and Dynamics*, 1–25. https://doi.org/10.1080/07391102.2020.1772111

Bhardwaj, V. K., Singh, R., Sharma, J., Rajendran, V., Purohit, R., & Kumar, S. (2020). Identification of bioactive molecules from tea plant as SARS-CoV-2 main protease inhibitors. *Journal of Biomolecular Structure and Dynamics*, 1–10. https://doi.org/10.1080/07391102.2020.1766572

Boopathi, S., Poma, A. B., & Kolandaivel, P. (2020). Novel 2019 Coronavirus Structure, Mechanism of Action, Antiviral drug promises and rule out against its treatment. *Journal of Biomolecular Structure & Dynamics*. 1-10. https://doi.org/10.1080/07391102.2020.1758788

Brooks, B. R., Bruccoleri, R. E., Olafson, B. D., States, D. J., Swaminathan, S., & Karplus, M. (1983). CHARMM: A program for macromolecular energy, minimization, and dynamics calculations. *Journal of Computational Chemistry*, *4*(2), 187–217. https://doi.org/10.1002/jcc.540040211

Burley, S. K., Berman, H. M., Bhikadiya, C., Bi, C., Chen, L., Di Costanzo, L., Christie, C., Dalenberg, K., Duarte, J. M., Dutta, S., Feng, Z., Ghosh, S., Goodsell, D. S., Green, R. K., Guranović, V., Guzenko, D., Hudson, B. P., Kalro, T., Liang, Y., … Zardecki, C. (2019). RCSB Protein Data Bank: Biological macromolecular structures enabling research and education in fundamental biology, biomedicine, biotechnology and energy. *Nucleic Acids Research*, *47*(D1), D464–D474. https://doi.org/10.1093/nar/gky1004

Chew, C. Y., Mar, A., Nikpour, M., & Saracino, A. M. (2020). Hydroxychloroquine in dermatology: New perspectives on an old drug. *Australasian Journal of Dermatology*, *61*(2), 1-10. https://doi.org/10.1111/ajd.13168

Choudhury, C. (2020). Fragment tailoring strategy to design novel chemical entities as potential binders of novel corona virus main protease. *Journal of Biomolecular Structure and Dynamics*, 1–14. https://doi.org/10.1080/07391102.2020.1771424

Das, S., Sarmah, S., Lyndem, S., & Singha Roy, A. (2020). An investigation into the identification of potential inhibitors of SARS-CoV-2 main

protease using molecular docking study. *Journal of Biomolecular Structure and Dynamics*. 1-11. https://doi.org/10.1080/07391102.2020.1763201

De Magalhães, C. S., Almeida, D. M., Barbosa, H. J. C., & Dardenne, L. E. (2014). A dynamic niching genetic algorithm strategy for docking highly flexible ligands. *Information Sciences*, *289*, 206–224. https://doi.org/10.1016/j.ins.2014.08.002

de Oliveira, O. V., Rocha, G. B., Paluch, A. S., & Costa, L. T. (2020). Repurposing approved drugs as inhibitors of SARS-CoV-2 S-protein from molecular modeling and virtual screening. *Journal of Biomolecular Structure and Dynamics*, 1–10. https://doi.org/10.1080/07391102.2020.1772885

Dennington, R., Keith, T., & Millam, J. (2009). *GaussView 5*. Semichem Inc.

Devaux, C. A., Rolain, J.-M., Colson, P., & Raoult, D. (2020). New insights on the antiviral effects of chloroquine against coronavirus: What to expect for COVID-19? *International Journal of Antimicrobial Agents*, *55*(5), 105938. https://doi.org/10.1016/j.ijantimicag.2020.105938

Elfiky, A. A. (2020a). Natural products may interfere with SARS-CoV-2 attachment to the host cell. *Journal of Biomolecular Structure and Dynamics*, 1–10. https://doi.org/10.1080/07391102.2020.1761881

Elfiky, A. A. (2020b). SARS-CoV-2 RNA dependent RNA polymerase (RdRp) targeting: An in silico perspective. *Journal of Biomolecular Structure and Dynamics*. 1-9. https://doi.org/10.1080/07391102.2020.1761882

Elfiky, A. A., & Azzam, E. B. (2020). Novel guanosine derivatives against MERS CoV polymerase: An in silico perspective. *Journal of Biomolecular Structure and Dynamics*, 1–9. https://doi.org/10.1080/07391102.2020.1758789

Elmezayen, A. D., Al-Obaidi, A., Şahin, A. T., & Yelekçi, K. (2020). Drug repurposing for coronavirus (COVID-19): In silico screening of known drugs against coronavirus 3CL hydrolase and protease enzymes. *Journal of Biomolecular Structure and Dynamics*, 1–13. https://doi.org/10.1080/07391102.2020.1758791

Enayatkhani, M., Hasaniazad, M., Faezi, S., Guklani, H., Davoodian, P., Ahmadi, N., Einakian, M. A., Karmostaji, A., & Ahmadi, K. (2020). Reverse vaccinology approach to design a novel multi-epitope vaccine candidate against COVID-19: An *in silico* study. *Journal of Biomolecular Structure and Dynamics*. 1-16. https://doi.org/10.1080/07391102.2020.1756411

Enmozhi, S. K., Raja, K., Sebastine, I., & Joseph, J. (2020). Andrographolide as a potential inhibitor of SARS-CoV-2 main protease: An in silico approach. *Journal of Biomolecular Structure and Dynamics*, 1–7. https://doi.org/10.1080/07391102.2020.1760136

Feller, S. E., Zhang, Y., Pastor, R. W., & Brooks, B. R. (1995). Constant pressure molecular dynamics simulation: The Langevin piston method. *The Journal of Chemical Physics*, *103*(11), 4613–4621. https://doi.org/10.1063/1.470648

Frisch, M. J., Trucks, G. W., Schlegel, H. B., Scuseria, G. E., Robb, M. A., Cheeseman, J. R., Scalmani, G., Barone, V., Mennucci, B., Petersson, G. A., Nakatsuji, H., Caricato, M., Li, X., Hratchian, H. P., Izmaylov, A. F., Bloino, J., Zheng, G., & Sonnenber, D. J. (2009). *Gaussian 09 A.02*. Gaussian, Inc. https://doi.org/111

Gasteiger, J., & Marsili, M. (1980). Iterative partial equalization of orbital electronegativity-a rapid access to atomic charges. *Tetrahedron*, *36*(22), 3219–3228. https://doi.org/10.1016/0040-4020(80)80168-2

Gautret, P., Lagier, J.-C., Parola, P., Hoang, V. T., Meddeb, L., Mailhe, M., Doudier, B., Courjon, J., Giordanengo, V., Vieira, V. E., Tissot Dupont, H., Honoré, S., Colson, P., Chabrière, E., La Scola, B., Rolain, J.-M., Brouqui, P., & Raoult, D. (2020). Hydroxychloroquine and azithromycin as a treatment of COVID-19: Results of an open-label non-randomized clinical trial. *International Journal of Antimicrobial Agents*, *56*(1), 105949. https://doi.org/10.1016/j.ijantimicag.2020.105949

Gullingsrud, J., Kosztin, D., & Schulten, K. (2001). Structural determinants of MscL gating studied by molecular dynamics simulations. *Biophysical Journal*, *80*(5), 2074–2081. https://doi.org/10.1016/S0006-3495(01)76181-4

Gupta, S., Singh, A. K., Kushwaha, P. P., Prajapati, K. S., Shuaib, M., Senapati, S., & Kumar, S. (2020). Identification of potential natural inhibitors of SARS-CoV2 main protease by molecular docking and simulation studies. *Journal of Biomolecular Structure and Dynamics*. 1-12. https://doi.org/10.1080/07391102.2020.1776157

Gyebi, G. A., Ogunro, O. B., Adegunloye, A. P., Ogunyemi, O. M., & Afolabi, S. O. (2020). Potential inhibitors of coronavirus 3-chymotrypsin-like protease (3CLpro): An in silico screening of alkaloids and terpenoids from African medicinal plants. *Journal of Biomolecular Structure and Dynamics*. 1-13. https://doi.org/10.1080/07391102.2020.1764868

Hasan, A., Paray, B. A., Hussain, A., Qadir, F. A., Attar, F., Aziz, F. M., Sharifi, M., Derakhshankhah, H., Rasti, B., Mehrabi, M., Shahpasand, K., Saboury, A. A., & Falahati, M. (2020). A review on the cleavage priming of the spike protein on coronavirus by angiotensin-converting enzyme-2 and furin. *Journal of Biomolecular Structure and Dynamics*. 1-9. https://doi.org/10.1080/07391102.2020.1754293

Hemida, M. G., & Ba Abduallah, M. M. (2020). The SARS-CoV-2 outbreak from a one health perspective. *One Health*, 100127. https://doi.org/10.1016/j.onehlt.2020.100127

Hendaus, M. A. (2020). Remdesivir in the treatment of coronavirus disease 2019 (COVID-19): A simplified summary. *Journal of Biomolecular Structure and Dynamics*, 1–6. https://doi.org/10.1080/07391102.2020.1767691

Hendaus, M. A., & Jomha, F. A. (2020). Covid-19 induced superimposed bacterial infection. *Journal of Biomolecular Structure and Dynamics*, 1–7. https://doi.org/10.1080/07391102.2020.1772110

Hu, B., Ge, X., Wang, L.-F., & Shi, Z. (2015). Bat origin of human coronaviruses. *Virology Journal*, *12*(1), 1-10. https://doi.org/10.1186/s12985-015-0422-1

Huang, J., & MacKerell, A. D. (2013). CHARMM36 all-atom additive protein force field: Validation based on comparison to NMR data. *Journal of Computational Chemistry*, *34*(25), 2135–2145. https://doi.org/10.1002/jcc.23354

Humphrey, W., Dalke, A., & Schulten, K. (1996). VMD: Visual molecular dynamics. *Journal of Molecular Graphics*, *14*(1), 33–38. https://doi.org/10.1016/0263-7855(96)00018-5

Islam, R., Parves, M. R., Paul, A. S., Uddin, N., Rahman, M. S., Mamun, A. A., Hossain, M. N., Ali, M. A., & Halim, M. A. (2020). A molecular modeling approach to identify effective antiviral phytochemicals against the main protease of SARS-CoV-2. *Journal of Biomolecular Structure and Dynamics*. 1-12. https://doi.org/10.1080/07391102.2020.1761883

Jin, Z., Du, X., Xu, Y., Deng, Y., Liu, M., Zhao, Y., Zhang, B., Li, X., Zhang, L., Peng, C., Duan, Y., Yu, J., Wang, L., Yang, K., Liu, F., Jiang, R., Yang, X., You, T., Liu, X., … Yang, H. (2020). Structure of Mpro from SARS-CoV-2 and discovery of its inhibitors. *Nature*, *582*(7811), 289–293. https://doi.org/10.1038/s41586-020-2223-y

Joshi, R. S., Jagdale, S. S., Bansode, S. B., Shankar, S. S., Tellis, M. B., Pandya, V. K., Chugh, A., Giri, A. P., & Kulkarni, M. J. (2020). Discovery of potential multi-target-directed ligands by targeting host-specific SARS-CoV-2 structurally conserved main protease. *Journal of Biomolecular Structure and Dynamics*, 1–16. https://doi.org/10.1080/07391102.2020.1760137

Kalé, L., Skeel, R., Bhandarkar, M., Brunner, R., Gursoy, A., Krawetz, N., Phillips, J., Shinozaki, A., Varadarajan, K., & Schulten, K. (1999). NAMD2: Greater Scalability for Parallel Molecular Dynamics. *Journal of Computational Physics*, *151*(1), 283–312. https://doi.org/10.1006/jcph.1999.6201

Khan, M. T., Ali, A., Wang, Q., Irfan, M., Khan, A., Zeb, M. T., Zhang, Y.-J., Chinnasamy, S., & Wei, D.-Q. (2020). Marine natural compounds as potents inhibitors against the main protease of SARS-CoV-2—a molecular dynamic study. *Journal of Biomolecular Structure and Dynamics*, 1–11. https://doi.org/10.1080/07391102.2020.1769733

Khan, R. J., Jha, R. K., Amera, G. M., Jain, M., Singh, E., Pathak, A., Singh, R. P., Muthukumaran, J., & Singh, A. K. (2020). Targeting SARS-CoV-2: A systematic drug repurposing approach to identify promising inhibitors against 3C-like proteinase and 2′-O-ribose methyltransferase. *Journal of Biomolecular Structure and Dynamics*. 1-14. https://doi.org/10.1080/07391102.2020.1753577

Khan, S. A., Zia, K., Ashraf, S., Uddin, R., & Ul-Haq, Z. (2020). Identification of chymotrypsin-like protease inhibitors of SARS-CoV-2 via integrated computational approach. *Journal of Biomolecular Structure and Dynamics*. 1-10. https://doi.org/10.1080/07391102.2020.1751298

Kumar, A., Choudhir, G., Shukla, S. K., Sharma, M., Tyagi, P., Bhushan, A., & Rathore, M. (2020). Identification of phytochemical inhibitors

against main protease of COVID-19 using molecular modeling approaches. *Journal of Biomolecular Structure and Dynamics*. 1-11. https://doi.org/10.1080/07391102.2020.1772112

Kumar, D., Kumari, K., Jayaraj, A., Kumar, V., Kumar, R. V., Dass, S. K., Chandra, R., & Singh, P. (2020). Understanding the binding affinity of noscapines with protease of SARS-CoV-2 for COVID-19 using MD simulations at different temperatures. *Journal of Biomolecular Structure and Dynamics*. 1-14. https://doi.org/10.1080/07391102.2020.1752310

Kumar, V., Dhanjal, J. K., Bhargava, P., Kaul, A., Wang, J., Zhang, H., Kaul, S. C., Wadhwa, R., & Sundar, D. (2020). Withanone and Withaferin-A are predicted to interact with transmembrane protease serine 2 (TMPRSS2) and block entry of SARS-CoV-2 into cells. *Journal of Biomolecular Structure and Dynamics*. 1-13. https://doi.org/10.1080/07391102.2020.1775704

Kumar, V., Dhanjal, J. K., Kaul, S. C., Wadhwa, R., & Sundar, D. (2020). Withanone and caffeic acid phenethyl ester are predicted to interact with main protease (M pro) of SARS-CoV-2 and inhibit its activity. *Journal of Biomolecular Structure and Dynamics*, 1–13. https://doi.org/10.1080/07391102.2020.1772108

Liu, H., & Hou, T. (2016). CaFE: A tool for binding affinity prediction using end-point free energy methods. *Bioinformatics (Oxford, England)*, *32*(14), 2216–2218. https://doi.org/10.1093/bioinformatics/btw215

Lobo-Galo, N., Terrazas-López, M., Martínez-Martínez, A., & Díaz-Sánchez, Á. G. (2020). FDA-approved thiol-reacting drugs that potentially bind into the SARS-CoV-2 main protease, essential for viral replication. *Journal of Biomolecular Structure and Dynamics*, 1–9. https://doi.org/10.1080/07391102.2020.1764393

MacKerell, A. D., Bashford, D., Bellott, M., Dunbrack, R. L., Evanseck, J. D., Field, M. J., Fischer, S., Gao, J., Guo, H., Ha, S., Joseph-McCarthy, D., Kuchnir, L., Kuczera, K., Lau, F. T., Mattos, C., Michnick, S., Ngo, T., Nguyen, D. T., Prodhom, B., … Karplus, M. (1998). All-Atom Empirical Potential for Molecular Modeling and Dynamics Studies of Proteins†. *The Journal of Physical Chemistry. B*, *102*(18), 3586–3616. https://doi.org/10.1021/jp973084f

Mahanta, S., Chowdhury, P., Gogoi, N., Goswami, N., Borah, D., Kumar, R., Chetia, D., Borah, P., Buragohain, A. K., & Gogoi, B. (2020). Potential anti-viral activity of approved repurposed drug against main protease of SARS-CoV-2: an in silico based approach. *Journal of Biomolecular Structure and Dynamics*. 1-10. https://doi.org/10.1080/07391102.2020.1768902

Mittal, L., Kumari, A., Srivastava, M., Singh, M., & Asthana, S. (2020). Identification of potential molecules against COVID-19 main protease through structure-guided virtual screening approach. *Journal of Biomolecular Structure and Dynamics*, 1–19. https://doi.org/10.1080/07391102.2020.1768151

Morris, G. M., Ruth, H., Lindstrom, W., Sanner, M. F., Belew, R. K., Goodsell, D. S., & Olson, A. J. (2009). Software news and updates AutoDock4 and AutoDockTools4: Automated docking with selective receptor flexibility. *Journal of Computational Chemistry*, *30*(16), 2785–2791. https://doi.org/10.1002/jcc.21256

Muralidharan, N., Sakthivel, R., Velmurugan, D., & Gromiha, M. M. (2020). Computational studies of drug repurposing and synergism of lopinavir, oseltamivir and ritonavir binding with SARS-CoV-2 protease against COVID-19. *Journal of Biomolecular Structure and Dynamics*. 1-6. https://doi.org/10.1080/07391102.2020.1752802

Pant, S., Singh, M., Ravichandiran, V., Murty, U. S. N., & Srivastava, H. K. (2020). Peptide-like and small-molecule inhibitors against Covid-19. *Journal of Biomolecular Structure & Dynamics*. 1-10. https://doi.org/10.1080/07391102.2020.1757510

Petrosillo, N., Viceconte, G., Ergonul, O., Ippolito, G., & Petersen, E. (2020). COVID-19, SARS and MERS: are they closely related? *Clinical Microbiology and Infection*, *26*(6), 729–734. https://doi.org/10.1016/j.cmi.2020.03.026

Pettersen, E. F., Goddard, T. D., Huang, C. C., Couch, G. S., Greenblatt, D. M., Meng, E. C., & Ferrin, T. E. (2004). UCSF Chimera - A visualization system for exploratory research and analysis. *Journal of Computational Chemistry*, *25*(13), 1605–1612. https://doi.org/10.1002/jcc.20084

Phillips, J. C., Braun, R., Wang, W., Gumbart, J., Tajkhorshid, E., Villa, E., Chipot, C., Skeel, R. D., Kalé, L., & Schulten, K. (2005). Scalable molecular dynamics with NAMD. *Journal of Computational Chemistry*, *26*(16), 1781–1802. https://doi.org/10.1002/jcc.20289

Quimque, M. T. J., Notarte, K. I. R., Fernandez, R. A. T., Mendoza, M. A. O., Liman, R. A. D., Lim, J. A. K., Pilapil, L., Ong, J., Pastrana, A. M., Khan, A., Wei, D. Q., & Macabeo, A. P. G. (2020). Virtual screening-driven drug discovery of SARS-CoV2 enzyme inhibitors targeting viral attachment, replication, post-translational modification and host immunity evasion infection mechanisms. *Journal of Biomolecular Structure and Dynamics*. 1-18. https://doi.org/10.1080/07391102.2020.1776639

Lu, R., Zhao, X., Li, J., Niu, P., Yang, B., Wu, H., Wang, W., Song, H., Huang, B., Zhu, N., Bi, Y., Ma, X., Zhan, F., Wang, L., Hu, T., Zhou, H., Hu, Z., Zhou, W., Zhao, L., … Tan, W. (2020). Genomic characterisation and epidemiology of 2019 novel coronavirus: implications for virus origins and receptor binding. *The Lancet*. 395(10224), 565–574. https://doi.org/10.1016/S0140-6736(20)30251-8

Rynes, R. I. (1988). Hydroxychloroquine treatment of rheumatoid arthritis. *The American Journal of Medicine*, *85*(4A), 18–22. https://doi.org/10.1016/0002-9343(88)90357-9

Santos, K. B., Guedes, I. A., Karl, A. L. M., & Dardenne, L. E. (2020). Highly Flexible Ligand Docking: Benchmarking of the DockThor Program on the LEADS-PEP Protein-Peptide Data Set. *Journal of Chemical Information and Modeling*, *60*(2), 667–683. https://doi.org/10.1021/acs.jcim.9b00905

Sarma, P., Shekhar, N., Prajapat, M., Avti, P., Kaur, H., Kumar, S., Singh, S., Kumar, H., Prakash, A., Dhibar, D. P., & Medhi, B. (2020). In-silico homology assisted identification of inhibitor of RNA binding against 2019-nCoV N-protein (N terminal domain). *Journal of Biomolecular Structure and Dynamics*. 1-9. https://doi.org/10.1080/07391102.2020.1753580

Sinha, S. K., Shakya, A., Prasad, S. K., Singh, S., Gurav, N. S., Prasad, R. S., & Gurav, S. S. (2020). An in-silico evaluation of different Saikosaponins for their potency against SARS-CoV-2 using NSP15 and fusion spike glycoprotein as targets. *Journal of Biomolecular Structure and Dynamics*, 1–12. https://doi.org/10.1080/07391102.2020.1762741

Sk, M. F., Roy, R., Jonniya, N. A., Poddar, S., & Kar, P. (2020). Elucidating biophysical basis of binding of inhibitors to SARS-CoV-2 main protease by using molecular dynamics simulations and free energy calculations. *Journal of Biomolecular Structure and Dynamics*, 1–13. https://doi.org/10.1080/07391102.2020.1768149

Sohrabi, C., Alsafi, Z., O'Neill, N., Khan, M., Kerwan, A., Al-Jabir, A., Iosifidis, C., & Agha, R. (2020). World Health Organization declares global emergency: A review of the 2019 novel coronavirus (COVID-19). *International Journal of Surgery*, *76*, 71–76. https://doi.org/10.1016/j.ijsu.2020.02.034

Tanenbaum, L., & Tuffanelli, D. L. (1980). Antimalarial Agents. *Archives of Dermatology*, *116*(5), 587–591. https://doi.org/10.1001/archderm.1980.01640290097026

Trott, O., & Olson, A. J. (2009). AutoDock Vina: Improving the speed and accuracy of docking with a new scoring function, efficient optimization, and multithreading. *Journal of Computational Chemistry*, *31*(2), 455–461. https://doi.org/10.1002/jcc.21334

Umesh, K. D., Selvaraj, C., Singh, S. K., & Dubey, V. K. (2020). Identification of new anti-nCoV drug chemical compounds from Indian spices exploiting SARS-CoV-2 main protease as target. *Journal of Biomolecular Structure and Dynamics*, 1–9. https://doi.org/10.1080/07391102.2020.1763202

Veeramachaneni, G. K., Thunuguntla, V. B. S. C., Bobbillapati, J., & Bondili, J. S. (2020). Structural and simulation analysis of hotspot residues interactions of SARS-CoV 2 with human ACE2 receptor. *Journal of Biomolecular Structure and Dynamics*, 1–11. https://doi.org/10.1080/07391102.2020.1773318

Wahedi, H. M., Ahmad, S., & Abbasi, S. W. (2020). Stilbene-based natural compounds as promising drug candidates against COVID-19. *Journal of Biomolecular Structure and Dynamics*. 1-10. https://doi.org/10.1080/07391102.2020.1762743

Wahie, S., & Meggitt, S. J. (2013). Long-term response to hydroxychloroquine in patients with discoid lupus erythematosus. *The British Journal of Dermatology*, *169*(3), 653–659. https://doi.org/10.1111/bjd.12378

Wang, L. F., & Eaton, B. T. (2007). Bats, civets and the emergence of SARS. *Current Topics in Microbiology and Immunology*, *315*, 325–344. https://doi.org/10.1007/978-3-540-70962-6_13

Weiner, S. J., Kollman, P. A., Case, D. A., Singh, U. C., Ghio, C., Alagona, G., Profeta, S., & Weiner, P. (1984). A new force field for molecular mechanical simulation of nucleic acids and proteins. *Journal of the American Chemical Society*, *106*(3), 765–784. https://doi.org/10.1021/ja00315a051

Zhang, L., Lin, D., Sun, X., Curth, U., Drosten, C., Sauerhering, L., Becker, S., Rox, K., & Hilgenfeld, R. (2020). Crystal structure of SARS-CoV-2 main protease provides a basis for design of improved a-ketoamide inhibitors. *Science*, *368*(6489), 409-412. https://doi.org/10.1126/science.abb3405

Zhang, T., Wu, Q., & Zhang, Z. (2020). Probable pangolin origin of SARS-CoV-2 associated with the COVID-19 outbreak. *Current Biology: CB*, *30*(7), 1346–1351.e2. https://doi.org/10.1016/j.cub.2020.03.022